A Bayesian approach to estimating the prehepatic insulin secretion rate

Andersen, Kim Emil; Højbjerre, Malene

Publication date:
2005

Document Version
Publisher's PDF, also known as Version of record

AALBORG UNIVERSITY

A Bayesian approach to estimating the prehepatic insulin secretion rate

by

Kim Emil Andersen and Malene Højbjerre

R-2005-35 December 2005

Department of Mathematical Sciences
Aalborg University
Fredrik Bajers Vej 7 G ▪ DK - 9220 Aalborg Øst ▪ Denmark
Phone: +45 96 35 80 80 ▪ Telefax: +45 98 15 81 29
URL: http://www.math.aau.dk

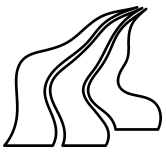

ISSN 1399–2503 ▪ On-line version ISSN 1601–7811

A Bayesian Approach to Estimating the Prehepatic Insulin Secretion Rate

KIM EMIL ANDERSEN AND MALENE HØJBJERRE

Department of Mathematical Sciences, Aalborg University,
Fredrik Bajers Vej 7G, DK-9220 Aalborg East
malene@math.aau.dk

SUMMARY

The prehepatic insulin secretion rate of the pancreatic β-cells is not directly measurable, since part of the secreted insulin is absorbed by the liver prior to entering the blood stream. However, C-peptide is co-secreted equimolarly and is not absorbed by the liver, allowing for the estimation of the prehepatic insulin secretion rate. We consider a stochastic differential equation model that combines both insulin and C-peptide concentrations in plasma to estimate the prehepatic insulin secretion rate. Previously this model has been analysed in an iterative deterministic set-up, where the time courses of insulin and C-peptide subsequently are used as known forcing functions. In this work we adopt a Bayesian graphical model to describe the unified model simultaneously. We develop a model that also accounts for both measurement error and process variability. The parameters are estimated by a Bayesian approach where efficient posterior sampling is made available through the use of Markov chain Monte Carlo methods. Hereby the ill-posed estimation problem inherited in the coupled differential equation model is regularized by the use of prior knowledge. The method is demonstrated on experimental data from an IntraVenous Glucose Tolerance Test (IVGTT) performed on six normal glucose-tolerant individuals.

Keywords: Bayesian graphical model; Markov chain Monte Carlo methods; Stochastic differential equation model; Insulin secretion rate, Insulin and C-peptide kinetics.

1 INTRODUCTION

Insulin resistance and failure of insulin secretion from the pancreatic β-cells are both major characteristics of type II diabetes, arguing that estimation of the pancreatic insulin secretion rate is of vital importance for a better understanding of the pathogenesis of type II diabetes. A gained knowledge about the pancreatic insulin secretion can be used in the development of a synthetic insulin for type II diabetes, where assessment of the endogenous insulin produced by the patients themselves is necessary to assess the therapeutic effect of the drug. In an artificial pancreas quantitative assessment of the true pancreatic insulin secretion is also required to emulate the human pancreas.

The insulin is secreted by the pancreatic β-cells, but prior to entering the blood stream, the insulin undergoes a large and variable liver extraction, whereby the prehepatic insulin secretion is not directly measurable in plasma. Fortunately, with the insulin, the hormone C-peptide is co-secreted equimolarly and is, in contrast to insulin, not significantly extracted by the liver. Thus the prehepatic insulin secretion rate may be estimated from C-peptide concentrations in plasma obtained from any glucose tolerance test, e.g. an IntraVenous Glucose Tolerance Test (IVGTT).

In an IVGTT study a bolus of glucose is administered intravenously into the blood stream and subsequently glucose, insulin and C-peptide concentrations in plasma are measured at pre-

specified time points. Estimation of prehepatic insulin secretion is then performed on the basis of the C-peptide concentrations traditionally by deconvolution as described in Eaton et al. (1980), where additional knowledge about the C-peptide kinetics is required. This is obtained from an initial same-day experiment, where plasma C-peptide concentrations are measured after a bolus of biosynthetic C-peptide. To avoid multiple experimental protocols Hovorka et al. (1994) propose using population C-peptide kinetics parameters adjusted for gender, age, height, weight and clinical status (normal, obese or Type II diabetic) obtained from an earlier study based on 250 patients. This approach has been implemented in the computer program ISEC (Hovorka, 1993; Hovorka et al., 1996), which is the most commonly used approach to estimate the prehepatic insulin secretion rate. However, these approaches solely use C-peptide concentrations in the estimation of the secretion rate, and do not take the insulin concentrations, which also contains valuable information about the quantity of interest, into considerations. Furthermore, deconvolution problems are often severely ill-posed implying that even small perturbations in data may result in unacceptably large distortions of the estimated solution (Hadamard, 1923). Therefore proper regularization within the reconstruction of the deconvolution problem is necessary, which has been addressed in Hovorka et al. (1996).

However, besides measuring the C-peptide concentrations in plasma the corresponding insulin concentrations are also obtained from the IVGTT study. Together these provide two sources of very useful information regarding the insulin secretion profile from only one single experimental protocol. Vølund et al. (1987) and Watanabe et al. (1989) present a combined model where both plasma insulin and C-peptide are used to derive estimates of the prehepatic insulin secretion. In this approach the plasma C-peptide kinetics is modelled by a single-compartmental model in order to minimize the number of parameters. However, as reported in Faber et al. (1978), the nature of C-peptide kinetics is two-compartmental, and the one-compartmental approximation only seems to hold under relative slow changes in the secretion rate. To comply with rapid fluctuations Watanabe et al. (1998) and Watanabe and Bergman (2000) extend the combined model to include a two-compartmental structure of the C-peptide kinetics without the need for an extra initial quantification of the C-peptide kinetics. The C-peptide kinetics parameters are estimated iteratively by considering the insulin and C-peptide successively as known, and then subsequently use them as forcing functions to estimate the prehepatic insulin secretion rate, modelled as a piecewise constant step function. Considering the insulin and C-peptide as known demands accurate data, or alternatively, a dense sampling scheme. A comprehensive review and comparison of the four approaches can be found in Kjems et al. (2001).

In this paper we consider the extended combined model of both insulin and two-compartmental C-peptide. We model both insulin and C-peptide as random variables to utilize the two sources of information simultaneously and allowing for error terms on the observations. The differential equations inherited in the model describing the C-peptide and insulin kinetics may not comply with the actual processes taking place inside the body, so we propose recasting the model in a stochastic setting, where error terms is imposed on the process increments (besides the error terms on the observations). This implies a far more complex and computationally intractable model though much more physiologically sound. However, by adopting a Bayesian graphical model (Lauritzen, 1996) the model can be analysed in a fully Bayesian approach based upon Markov chain Monte Carlo (MCMC) methods (Brooks, 1998; Robert and Casella, 1999). We hereby regularize the ill-posed estimation problem by using suitable *prior*

knowledge about the parameters. To be able to perform inference, distributional assumptions are needed for the secretion rate. We model this as a superposition of scaled gamma densities and develop a method for providing posterior inference of the prehepatic insulin secretion rate together with corresponding credible intervals. The method is validated via a simulation study and we demonstrate it afterwards on experimental IVGTT data from six normal-glucose tolerant individuals, concluding that the methodology for assessing the secretory rate presented here appears to be efficient and reliable.

We begin in Section 2 with a presentation of the data and the extended combined model of insulin and C-peptide. In Section 3 we construct the model as a Bayesian graphical model and in Section 4 we provide details of the statistical methodology used, together with a simulation study to demonstrate the utility and robustness of the proposed method. We present our results on experimental data in Section 5 and a discussion of the achieved results are provided in Section 6.

2 Data and Model

In an IVGTT study a bolus of glucose is administered intravenously to individuals for the purpose of recording the responding glucose, insulin and C-peptide concentrations in plasma over a pre-specified time period, normally 240 minutes. Corresponding basal glucose, insulin and C-peptide concentrations prior to the bolus are also recorded, traditionally for 60 minutes. Experimental data for a normal glucose tolerant individual are depicted in Figure 1.

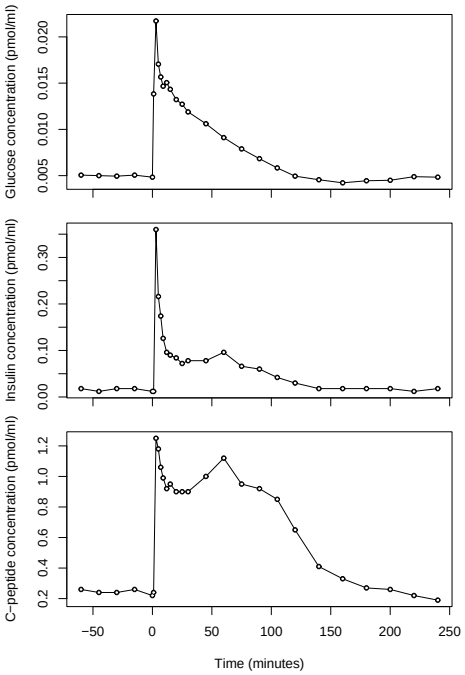

Figure 1: Glucose, insulin and C-peptide concentrations in plasma frequently sampled over 240 minutes after an intravenous glucose injection given to a normal glucose tolerant individual. Shown is also observations recorded 60 minutes prior to administration of glucose.

It is apparent that the injected glucose load immediately elevates the glucose concentration in plasma initiating an equimolar secretion of insulin and C-peptide from the pancreatic β-cells. Prior to entering the blood stream the insulin undergoes a large liver extraction, whereas C-peptide is not extracted significantly. The provoked hyperglycemia in plasma induces a peak of both insulin and C-peptide concentrations in plasma, and the increased insulin level raises the glucose uptake in muscles, liver and adipose tissue. This lowers the glucose concentration in plasma, affecting the β-cells to secrete less insulin, whereby a feedback effect arises. By approximately 2 hours, the glucose concentration is normalized, and in the following hour a moderate undershoot is observed. After approximately 3 hours, it is usually found that the perturbed concentrations essentially have returned to normal. Depending upon the state of the tested individual, the glucose, insulin and C-peptide concentrations may vary considerably from the response shown in Figure 1. Note that we, in this work, do not not utilize the corresponding glucose concentrations, even though it also indirectly contains valuable information about the secretion rate.

The extended combined model proposed in Watanabe et al. (1998) describes the kinetics of both insulin and C-peptide during the single experiment of an IVGTT study. The model is based upon the assumptions that the prehepatic secretion of both insulin and C-peptide is equimolar and that the fraction of insulin extracted by the liver is constant during the experiment. The model can be represented by the compartmental system illustrated in Figure 2, where a single compartment is sufficient for the insulin, in contrast to the C-peptide, where an additional extravascular compartment is required as stated by Faber et al. (1978).

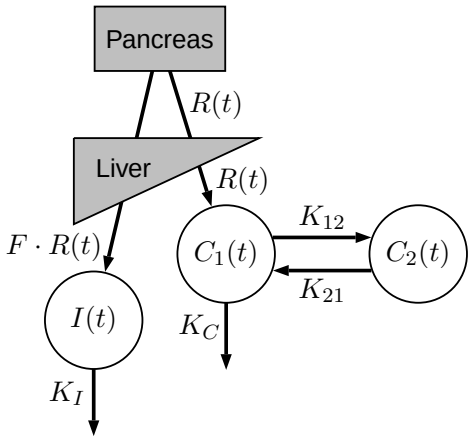

Figure 2: The extended combined model describing the insulin and C-peptide kinetics during an intravenous glucose tolerance test.

To time t let the concentration in the plasma insulin compartment be denoted by $I(t)$ [pmol/ml], the plasma C-peptide compartment by $C_1(t)$ [pmol/ml] and the extravascular C-peptide compartment by $C_2(t)$ [pmol/ml]. Furthermore, let $R(t)$ [pmol/min] denote the equimolar insulin and C-peptide secretion rate performed by the β-cells and assume that the constant fraction of insulin extracted by the liver is $1 - F$, whereby $F \cdot R(t)$ represents the rate by which the insulin surviving liver extraction is distributed into the blood circulating system. For C-peptide the rate $R(t)$ remains unchanged during the transportation through the liver.

The kinetics of the system can then be described by the following set of inhomogeneous linearly coupled differential equations

$$\begin{aligned} V_I\dot{I}(t) &= FR(t) - K_I I(t)V_I, & I(0) &= I^b, \\ V_{C_1}\dot{C}_1(t) &= R(t) - (K_{12}+K_C)C_1(t)V_{C_1} + K_{21}C_2(t)V_{C_2}, & C_1(0) &= C_1^b, \\ V_{C_2}\dot{C}_2(t) &= K_{12}C_1(t)V_{C_1} - K_{21}C_2(t)V_{C_2}, & C_2(0) &= C_2^b, \end{aligned} \tag{2.1}$$

where V_I, V_{C_1} and V_{C_2} are the distribution volumes of the plasma insulin, the plasma C-peptide and the extravascular C-peptide, respectively, and the initial concentrations in the three compartments are equal to their respective base levels, i.e. I^b, C_1^b and C_2^b. The parameters K_{12} and K_{21} are the transfer rates between the two C-peptide compartments, and K_I and K_C are the elimination rates from the plasma compartments of insulin and C-peptide, respectively. The secretion rate per unit distribution volume of C-peptide in plasma is defined as $r(t) = R(t)/V_{C_1}$, which is actually the quantity of interest. Introducing $f = F \cdot V_{C_1}/V_I$ as the prehepatic transition fraction normalized according to the ratio of the plasma C-peptide and plasma insulin distribution volumes and $V_{12} = V_{C_1}/V_{C_2}$ as the fraction of the two C-peptide distribution volumes the differential equations becomes

$$\begin{aligned} \dot{I}(t) &= fr(t) - K_I I(t), & I(0) &= I^b, \\ \dot{C}_1(t) &= r(t) - (K_{12}+K_C)C_1(t) + K_{21}/V_{12}C_2(t), & C_1(0) &= C_1^b, \\ \dot{C}_2(t) &= K_{12}V_{12}C_1(t) - K_{21}C_2(t), & C_2(0) &= C_2^b, \end{aligned} \tag{2.2}$$

Note that by considering the model (2.2) in steady state we easily obtain the following three parameter dependencies

$$r^b = K_C C_1^b, \quad f = \frac{K_I I^b}{K_C C_1^b} \quad \text{and} \quad C_2^b = \frac{K_{12}}{K_{21}} V_{12} C_1^b,$$

where r^b denotes the basal insulin secretion rate. In order to ascertain a model consistent within its parameterization we thus represent the basal levels r^b and C_2^b and the prehepatic transition factor f by the remaining model parameters.

The assumption that the insulin and the C-peptide are co-secreted equimolarly implies that the insulin secretion rate, $r(t)$, in the above equations can be factored out. Watanabe et al. (1998) exploits this, to obtain a set of equations that relates the plasma insulin and plasma C-peptide without the need for the actual secretion rate. The kinetics parameters are then estimated iteratively assuming successively that the insulin and C-peptide are known as forcing functions. Afterwards the insulin secretion rate is estimated by deconvolution on the basis of these parameters. Hereby the identification of the secretion rate is purely data-driven without error terms on the observations. Besides, it does not consider the whole system as an integrated system of both insulin and C-peptide, which it is by nature. Due to expected fluctuations from the underlying processes inside the body we believe that the model also should be regarded as a stochastic differential equation model to mimic this.

However, solving the three coupled differential equations in (2.2) simultaneously (deterministic or stochastic) still remains a highly ill-posed estimation problem, i.e. even small perturbations in the observations of the insulin and C-peptide may result in unacceptably large

distortions of the estimated solution. Therefore proper regularization in the reconstruction of the insulin secretion rate is called for. Regularization is often done by imposing certain regularity conditions on the solution space, which in a likelihood approach is equivalent to using a penalized likelihood function, where the solution space is reduced by introducing a penalty function for implausible solutions. In a Bayesian approach it is tackled by using a prior distribution on the parameters, whereby the implausible parameters automatically are penalized. The Bayesian approach inherits other advantages, e.g. the availability of computational tools such as MCMC methods which allow for the construction and analysis of suitable complex models without the need for simplifying assumptions. We utilize this ability by adopting a Bayesian graphical model to illustrate the complicated relationship among the parameters in the stochastic differential equation model defined by (2.2). The Bayesian graphical model is derived in the following section.

3 The Insulin and C-peptide Model as a Bayesian Graphical Model

The deterministic differential equation model defined in (2.2) may not comply with the actual insulin and C-peptide processes inside the body. By introducing Brownian motion fluctuations, say B^I, B^{C_1} and B^{C_2}, we can model such possible deviations, whereby a stochastic version of the model is expressed as

$$\begin{aligned} dI(t) &= \big(fr(t) - K_I I(t)\big)dt + \tau_I^{-1/2} dB^I(t), \\ dC_1(t) &= \big(r(t) - (K_{12} + K_C)C_1(t) + K_{21}/V_{12} C_2(t)\big)dt + \tau_{C_1}^{-1/2} dB^{C_1}(t), \\ dC_2(t) &= \big(K_{12} V_{12} C_1(t) - K_{21} C_2(t)\big)dt + \tau_{C_2}^{-1/2} dB^{C_2}(t), \end{aligned}$$

where τ_I, τ_{C_1} and τ_{C_2} denote the reciprocal variances (precisions) of the introduced Brownian motions. This differential form of the stochastic model can by simple integration be reformulated as an equivalent set of integral equations, e.g. for the insulin process, as

$$I(t_k) - I(t_{k-1}) = \int_{t_{k-1}}^{t_k} (fr(t) - K_I I(t))dt + \tau_I^{-1/2}(B^I(t_k) - B^I(t_{k-1})),$$

where $t_k - t_{k-1} > 0$ is a suitably small time span. The involved unknown integral can be approximated by the product between its width and its left end point, i.e.

$$I(t_k) = I(t_{k-1}) + (t_k - t_{k-1})\big(fr(t_{k-1}) - K_I I(t_{k-1})\big) + \epsilon^I(t_k - t_{k-1}),$$

where the random process $\epsilon^I(t_k - t_{k-1}) = \tau_I^{-1/2}(B^I(t_k) - B^I(t_{k-1}))$ is well-known to depend only on the time interval $t_k - t_{k-1}$ following a normal distribution with mean zero and variance $\tau_I^{-1}(t_k - t_{k-1})$.

Similarly the differential equations for the C-peptide processes can be reformulated, and using t as subscript the joint stochastic model of both insulin and C-peptide can be expressed as

$$\begin{aligned} I_{t_k} &= h^I(I_{t_{k-1}}, r_{t_{k-1}}) + \epsilon^I(t_k - t_{k-1}), \\ C_{1_{t_k}} &= h^{C_1}(C_{1_{t_{k-1}}}, C_{2_{t_{k-1}}}, r_{t_{k-1}}) + \epsilon^{C_1}(t_k - t_{k-1}), \\ C_{2_{t_k}} &= h^{C_2}(C_{1_{t_{k-1}}}, C_{2_{t_{k-1}}}, r_{t_{k-1}}) + \epsilon^{C_2}(t_k - t_{k-1}), \end{aligned}$$

with

$$
\begin{aligned}
h^I(I_{t_{k-1}}, r_{t_{k-1}}) &= I_{t_{k-1}} + (t_k - t_{k-1})\big(f r_{t_{k-1}} - K_I I_{t_{k-1}}\big),\\
h^{C_1}(C_{1_{t_{k-1}}}, C_{2_{t_{k-1}}}, r_{t_{k-1}}) &= C_{1_{t_{k-1}}} + (t_k - t_{k-1})\big(r_{t_{k-1}} - (K_{12}+K_C)C_{1_{t_{k-1}}} + K_{21}/V_{12} C_{2_{t_{k-1}}}\big),\\
h^{C_2}(C_{1_{t_{k-1}}}, C_{2_{t_{k-1}}}, r_{t_{k-1}}) &= C_{2_{t_{k-1}}} + (t_k - t_{k-1})\big(K_{12} V_{12} C_{1_{t_{k-1}}} - K_{21} C_{2_{t_{k-1}}}\big),
\end{aligned}
$$

where the functional dependencies of the parameters f, K_I, K_C K_{12}, K_{21} and V_{12} are suppressed.

The conditional distributions for the processes I_{t_k}, $C_{1_{t_k}}$ and $C_{2_{t_k}}$ are hereby given as

$$
\begin{aligned}
I_{t_k} \,|\, I_{t_{k-1}}, r_{t_{k-1}}, \tau_I &\sim \mathcal{N}(h^I(I_{t_{k-1}}, r_{t_{k-1}}), \tau_I^{-1}(t_k - t_{k-1})),\\
C_{1_{t_k}} \,|\, C_{1_{t_{k-1}}}, C_{2_{t_{k-1}}}, r_{t_{k-1}}, \tau_{C_1} &\sim \mathcal{N}(h^{C_1}(C_{1_{t_{k-1}}}, C_{2_{t_{k-1}}}, r_{t_{k-1}}), \tau_{C_1}^{-1}(t_k - t_{k-1})),\\
C_{2_{t_k}} \,|\, C_{1_{t_{k-1}}}, C_{2_{t_{k-1}}}, r_{t_{k-1}}, \tau_{C_2} &\sim \mathcal{N}(h^{C_2}(C_{1_{t_{k-1}}}, C_{2_{t_{k-1}}}, r_{t_{k-1}}), \tau_{C_2}^{-1}(t_k - t_{k-1})).
\end{aligned}
\tag{3.1}
$$

We can see that there is a relationship between the insulin/C-peptide processes and the process underlying the secretion rate. Therefore distributional assumptions for r_{t_k} is necessary to perform fully Bayesian inference. In Watanabe et al. (1998) the secretion rate is modelled by a stepwise constant function with variable step length depending upon the applied sampling scheme, i.e. it is impossible for the secretion rate to vary between any two successive sample points.

Let $r^b \geq 0$ denote the basal insulin secretion rate. Then we propose modelling the deviation from basal insulin secretion level by imposing a scaled sum of weighted gamma densities, i.e. we represent the mean structure of $r(t)$ by

$$
h^r(t) = r^b + \kappa \sum_{k=1}^{K} w_k \frac{\beta_k^{\alpha_k}}{\Gamma(\alpha_k)} t^{\alpha_k - 1} e^{-\beta_k t}, t \geq 0.
$$

Prior to administering the bolus, $t < 0$, we let $h_r(t) = r^b$. Let $\Upsilon = (\kappa, \alpha, \beta, w)$ with $\kappa > 0$, $\alpha = (\alpha_1, \ldots, \alpha_K), \alpha_k > 1$, $\beta = (\beta_1, \ldots, \beta_K), \beta_k > 0$ and $w = (w_1, \ldots, w_K), w_k \in \mathbb{R}$ subject to the condition $\sum_{k=1}^{K} w_k = 1$. Note that the weights themselves are not confined to be strictly positive allowing the insulin secretion rate to fall beneath the basal level r^b. Hereby the conditional distribution for the secretion process r_{t_k} is modelled as

$$
r_{t_k} \,|\, t_k, \tau_r \sim \mathcal{N}(h^r(t_k), \tau_r^{-1}). \tag{3.2}
$$

where the functional dependency on the parameters r^b and Υ have been suppressed for notational convenience.

The conditional distributions in (3.1) and (3.2), defining the model, can be interpreted as parent-child distributions in a directed graphical model. In a directed graphical model the quantities of a model are represented by vertices and a direct influence from one quantity to another is illustrated by a directed edge. Hereby the model in (3.1) and (3.2) can be illustrated by the graphical model provided in Figure 3. In the graph we have omitted the parameter vertices due to the complexity of the graph, but added the vertices $I^o_{t_k}$ and $C^o_{1_{t_k}}$ to represent the random variables corresponding to the observations of the plasma insulin and C-peptide for specific time points t_k. A general treatment of graphical models can be found in Lauritzen (1996).

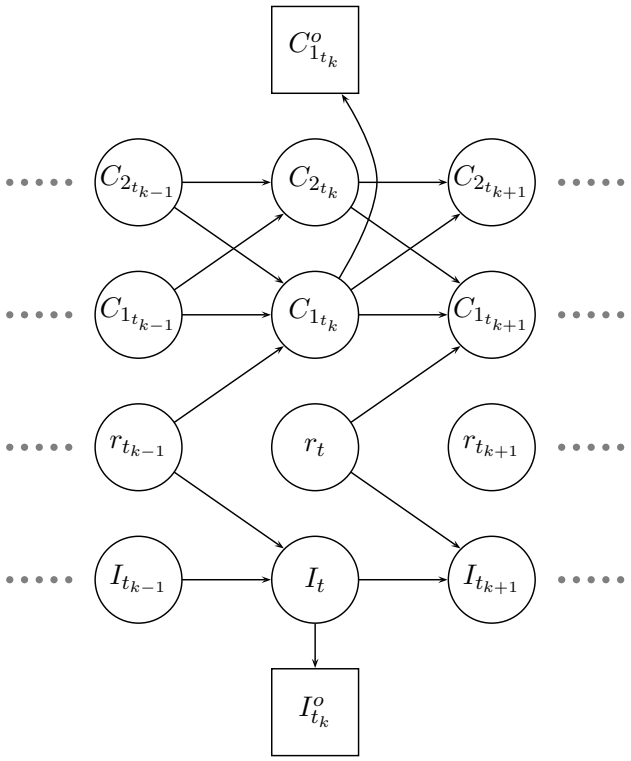

Figure 3: Directed acyclic graph illustrating the statistical dependencies for the latent processes, I, C_1, C_2 and r, and the observed processes I^o and C^o_1. The observed quantities are illustrated by rectangles and the unobserved quantities are illustrated by circles. Parameter dependencies are not shown due to the complexity of the graph.

The measurement error on the observation processes I^o_t and $C^o_{1_t}$ is known to increase with the mean. Consequently we model the measurement error on $\log I^o_t$ and $\log C^o_{1_t}$ by two independent random white noise processes; ϵ^{I^o} and $\epsilon^{C^o_1}$ with precisions τ_{I^o} and $\tau_{C^o_1}$, respectively. Consequently the distributional assumptions for $I^o_{t_k}$ and $C^o_{1_{t_k}}$ are

$$\begin{aligned} \log I^o_{t_k} \mid I_{t_k}, \tau_{I^o} &\sim \mathcal{N}(\log I_{t_k}, \tau^{-1}_{I^o}), \\ \log C^o_{1_{t_k}} \mid C_{1_{t_k}}, \tau_{C^o_1} &\sim \mathcal{N}(\log C_{1_{t_k}}, \tau^{-1}_{C^o_1}). \end{aligned} \tag{3.3}$$

Note that the model is constructed such that the mean structures of the observations depend on the underlying non-observable latent system processes of $I_{t_k}, C_{1_{t_k}}, C_{2_{t_k}}$ and r_{t_k} defined in (3.1) and (3.2), respectively.

The unobserved quantities of the model is collected into two subsets; the parameters

$$\Omega = (\Upsilon, K_I, K_C, K_{12}, K_{21}, V_{12}, I^b, C^b_1, \tau_I, \tau_{C_1}, \tau_{C_2}, \tau_r, \tau_{I^o}, \tau_{C^o_1})$$

and the four latent processes

$$\Psi = \{I_{t_k}, C_{1_{t_k}}, C_{2_{t_k}}, r_{t_k}\}_{t_k \in \Lambda},$$

where Λ denotes the time points chosen for approximating the underlying processes. Recall that r^b, C_2^b and f are functions of Ω and thus need no further considerations.

The observations are represented by $\Phi = \{I^o_{t_k}, C^o_{1_{t_k}}\}_{t_k \in \mathcal{T}}$, where $\mathcal{T} \subseteq \Lambda$ denotes the set of actual observation times. The posterior distribution of the unobserved quantities given the observed quantities can then up to a constant be expressed as

$$p(\Omega, \Psi \mid \Phi) \propto p(\Phi \mid \Omega, \Psi) p(\Psi \mid \Omega) p(\Omega), \tag{3.4}$$

where $p(\Omega)$ represents our beliefs about the parameters before having observed any data, i.e. the prior distribution, and $p(\Psi \mid \Omega)$ and $p(\Phi \mid \Omega, \Psi)$ form the likelihood determined by (3.1) – (3.3).

Using the recursive factorization property of a directed graphical model it can easily be derived that

$$\begin{aligned} p(\Psi \mid \Omega) = \prod_{t_k \in \Lambda} \Big[& p(I_{t_k} \mid I_{t_{k-1}}, r_{t_{k-1}}, \tau_I) p(C_{1_{t_k}} \mid C_{1_{t_{k-1}}}, C_{2_{t_{k-1}}}, r_{t_{k-1}}, \tau_{C_1}) \\ & \times p(C_{2_{t_k}} \mid C_{1_{t_{k-1}}}, C_{2_{t_{k-1}}}, r_{t_{k-1}}, \tau_{C_2}) p(r_{t_k} \mid r_{t_{k-1}}, \tau_r) \Big] \\ \propto & (\tau_I \tau_{C_1} \tau_{C_2} \tau_r)^{N/2} \exp\{-V(\Psi, \Omega)\}, \end{aligned} \tag{3.5}$$

where $N = |\Lambda|$ denotes the number of elements in Λ and the posterior potential V is given by

$$V(\Psi, \Omega) = \frac{1}{2} \sum_{t_k \in \Lambda} \left\{ \frac{\tau_I (I_{t_k} - h^I_{t_k})^2 + \tau_{C_1} (C_{1_{t_k}} - h^{C_1}_{t_k})^2 + \tau_{C_2} (C_{2_{t_k}} - h^{C_2}_{t_k})^2}{t_k - t_{k-1}} + \tau_r (r_{t_k} - h^r_{t_k})^2 \right\},$$

with $h^I_{t_k} = h^I(I_{t_{k-1}}, r_{t_{k-1}})$, $h^{C_1}_{t_k} = h^{C_1}(C_{1_{t_{k-1}}}, C_{2_{t_{k-1}}}, r_{t_{k-1}})$, $h^{C_2}_{t_k} = h^{C_2}(C_{1_{t_{k-1}}}, C_{2_{t_{k-1}}}, r_{t_{k-1}})$ and $h^r_{t_k} = h^r(r_{t_{k-1}})$.

Similarly, for the random variables corresponding to the observations of insulin and C-peptide it is easily seen that

$$\begin{aligned} p(\Phi \mid \Omega, \Psi) &= \prod_{t_k \in \mathcal{T}} p(I^o_{t_k} \mid I_{t_k}, \tau_{I^o}) p(C^o_{1_{t_k}} \mid C_{1_{t_k}}, \tau_{C_1{}^o}) \\ &\propto (\tau_{I^o} \tau_{C_1{}^o})^{M/2} \exp\{-W(\Phi, \Omega, \Psi)\}, \end{aligned} \tag{3.6}$$

where $M = |\mathcal{T}|$ denotes the number of observations and

$$W(\Phi, \Omega, \Psi) = \frac{1}{2} \sum_{t_k \in \mathcal{T}} \tau_{I^o} (\log I^o_{t_k} - \log I_{t_k})^2 + \tau_{C_1{}^o} (\log C^o_{1_{t_k}} - \log C_{1_{t_k}})^2.$$

For the parameters in Ω we assume that they are independent a priori and that each of the system parameters $K_I, K_C, K_{12}, K_{21}, V_{12}, I^b$ and C_1^b are normally distributed and that the positive precisions $\tau_I, \tau_{C_1}, \tau_{C_2}, \tau_r, \tau_{I^o}$ and $\tau_{C_1^o}$ each has a Gamma prior. However, the parameter vector Υ representing the secretion rate also needs prior specification. Thus we let

$$\boldsymbol{\Xi} = \Big\{ \Upsilon \mid \kappa > 0, \alpha_k > 1, \beta_k > 0 \text{ for } k = 1, \ldots, K, \sum_{k=1}^{K} w_k = 1 \text{ and } h^r(t) \geq 0 \text{ for } t \geq 0 \Big\}$$

denote the set of allowable insulin secretion configurations. For Υ we assume that the prior distribution p on Ξ has a density which satisfies

$$p(\Upsilon) \propto p_1(1-p_1)^{K-1}p(\kappa)\mathbb{1}(\Upsilon \in \Xi)\prod_{k=1}^{K} p(w_k)p(\alpha_k/\beta_k)p(\alpha_k/\beta_k^2)$$

where p_1 is a user specified parameter denoting the probability that $K = 1$ and $\mathbb{1}$ denotes the indicator function. Here $p(w_k)$, $p(\alpha_k/\beta_k)$ and $p(\alpha_k/\beta_k^2)$ denote simple uniform priors on the weights, means and variances used for the description of $r(t)$. Note that a geometric prior is imposed on the number of gamma densities in $r(t)$ conveniently allowing us to control the degree of fit via e.g. the Akaike information criterion (AIC) or the Bayesian information criterion (BIC), see Poland and Shachter (1994) for details. Consequently the prior distribution of all the unknown parameters Ω can be found as the product of $p(\Upsilon)$ and normal and gamma densities as

$$\begin{aligned} p(\Omega) = p(\Upsilon)p(K_I)p(K_C)p(K_{12})p(K_{21})p(V_{12})p(I^b)p(C_1^b) \\ \times p(\tau_I)p(\tau_{C_1})p(\tau_{C_2})p(\tau_r)p(\tau_{I^o})p(\tau_{C_1^o}) \end{aligned}$$

4 Simulation Based Inference

Having specified the posterior distribution $p(\Omega, \Psi \mid \Phi)$ in (3.4) by means of the a priori beliefs and the actual observed data we need an efficient and reliable technique to facilitate posterior inference about the parameters of interest. We propose using MCMC methods which provide an alternative integration technique whereby e.g. posterior means are estimated by constructing an irreducible Markov chain $\{(\Omega_1, \Psi_1), (\Omega_2, \Psi_2), \ldots\}$ with stationary distribution $p(\Omega, \Psi \mid \Phi)$.

In order to efficiently investigate the state space we propose using different transition types allowing for within model moves and between model moves. The within model moves leave the number of used scaled gamma densities, K, invariant and are thus concerned with simple Metropolis–Hastings random walk updates. However, the between model moves alters K and thus the trans dimensional MCMC transition methodology (Green, 1995) is required to allow for jumps between models.

The construction of the proposed within model and between model updating mechanisms proposed for assessment of the insulin secretion rate are obviously of crucial importance. In particular, the updating of the parameters α and β is expected to be troublesome due to high within and between correlations. In order to obtain a Markov chain with adequate properties we propose reparameterizing the insulin secretion model in terms of the means and variances in the entering gamma densities. Thus we update the mean $m_k = \alpha_k/\beta_k$ leaving the variance $v_k = \alpha_k/\beta_k^2$ invariant and vice versa. Consequently the model for $r(t)$ in terms of $(m_1, \ldots, m_K)$ and $(v_1, \ldots, v_K)$ becomes

$$h^r(t) = r^b + \kappa \sum_{k=1}^{K} w_k \frac{(m_k/v_k)^{m_k^2/v_k}}{\Gamma\left(m_k^2/v_k\right)} t^{m_k^2/v_k - 1} e^{-m_k/v_k t}.$$

Implementational details on the proposed transitions are provided below.

4.1 WITHIN MODEL MOVES

We propose using a series of within model moves in which single parts of the entire state vector Ω is updated. Thus a candidate Ω'_j is proposed from a symmetric proposal distribution $q(\Omega_j; \Omega'_j)$. However, there is a strong natural inter-relationship between the parameters Ω and the processes Ψ and it was found that an adequately blocked Metropolis–Hastings updating mechanism was required to ensure a Markov chain with good mixing properties. Consequently Ψ'_j is proposed from $p(\Psi_j \mid \Omega'_j)$ and subsequently this joint proposal (Ω'_j, Ψ'_j) is accepted with probability

$$\alpha(\Omega_j, \Psi_j; \Omega'_j, \Psi'_j) = \min\left\{1, \frac{p(\Phi \mid \Omega'_j, \Psi'_j)p(\Psi'_j \mid \Omega'_j)p(\Omega'_j)}{p(\Phi \mid \Omega_j, \Psi_j)p(\Psi_j \mid \Omega_j)p(\Omega_j)}\right\}.$$

4.2 BETWEEN MODEL MOVES

Suppose a between model move is attempted and that the number of entering gamma densities in $r(t)$ is K. A transition of this type requires a reversible jump MCMC update which we implement as follows. First we select a new model to jump to, i.e. we choose with equal probability between the introduction of a new contribution $(w_{K+1}, m_{K+1}, v_{K+1})$ to $r(t)$ or the removal of one of the K existing (w_k, m_k, v_k) contributions. Thus the proposal Ω'_j is generated from a deterministic injective function $g(\Omega_j, \boldsymbol{u})$, where $\boldsymbol{u}$ is a continuous random vector with density $q(\boldsymbol{u})$. The acceptance probability for a reversible jump transition of this type is given by

$$\alpha(\Omega_j,\Psi_j; \Omega'_j,\Psi'_j) = \min\left\{1, \frac{p(\Phi \mid \Omega'_j, \Psi'_j)p(\Psi'_j \mid \Omega'_j)p(\Omega'_j)r_{m'}(\Omega'_j)}{p(\Phi \mid \Omega_j, \Psi_j)p(\Psi_j \mid \Omega_j)p(\Omega_j)r_m(\Omega_j)q(\boldsymbol{u})}\left|\frac{\partial g(\Omega_j, \boldsymbol{u})}{\partial(\Omega_j, \boldsymbol{u})}\right|\right\}, \quad (4.1)$$

where $r_m(\Omega_j)$ and $r_{m'}(\Omega'_j)$ denotes the probability of choosing trans dimensional move type m when in state Ω and the reverse move to m' when in Ω', respectively. Note that the final term in the above ratio is the Jacobian arising from the change of variables associated with moving from one space to the other.

Introducing a new contribution completely at random or removing one of the existing contributions performs poorly and resulted in extremely small acceptance probabilities and thus a more sophisticated between model transition was needed. As an alternative to the birth and death move types we instead propose split and merge move types. Assume that we have decided to attempt a split model move type. We do this by picking one contribution (w_k, m_k, v_k) uniformly between the K existing contributions. Denote this probability by $r_{\text{split}} = 1/K$. This contribution is split into two new contributions according to the injective map

$$g : (w_k, m_k, v_k) \longmapsto \begin{cases} (w_k - w_{K+1}, m_k - m_{K+1}, v_k - v_{K+1}) \\ (w_{K+1}, m_{K+1}, v_{K+1}), \end{cases}$$

where the random vector $\boldsymbol{u} = (w_{K+1}, m_{K+1}, v_{K+1})$ denotes the new contribution to $r(t)$. We will assume that $\boldsymbol{u}$ comes from a uniform distribution $q(\boldsymbol{u})$ on the product space $[-l_w, l_w] \times [0, l_m] \times [0, l_v]$, i.e. $q(\boldsymbol{u}) = 1/(l_w^2 l_m l_v)$. Note that the probability for performing the reverse

move is $r_{\text{merge}} = 2/(K(K+1))$. The Jacobian term $\left|\partial g(\Omega, \boldsymbol{u})/\partial(\Omega, \boldsymbol{u})\right|$ in (4.1) is simply one, hence the acceptance probability for performing a split operation becomes

$$\alpha_{\text{split}}(\Omega_j, \Psi_j; \Omega'_j, \Psi'_j) = \min\left\{1, \frac{p(\Phi \mid \Omega'_j, \Psi'_j)p(\Psi'_j \mid \Omega'_j)p(\Omega'_j)}{p(\Phi \mid \Omega_j, \Psi_j)p(\Psi_j \mid \Omega_j)p(\Omega_j)} \frac{2l_w^2 l_m l_v}{K+1}\right\}.$$

The death of a contribution is performed similarly, with any two of the K contributions being proposed for merging. A move which is subsequently accepted with probability

$$\alpha_{\text{merge}}(\Omega_j, \Psi_j; \Omega'_j, \Psi'_j) = \min\left\{1, \frac{p(\Phi \mid \Omega'_j, \Psi'_j)p(\Psi'_j \mid \Omega'_j)p(\Omega'_j)}{p(\Phi \mid \Omega_j, \Psi_j)p(\Psi_j \mid \Omega_j)p(\Omega_j)} \frac{K}{2l_w^2 l_m l_v}\right\}.$$

Evidently the between model moves are the minimum requirement for traversing the entire state space. However, supplementing the between model moves with within model moves allows for a more rapid exploration of the state space.

4.3 Fine Tuning

To guarantee satisfactory performance of the proposed MCMC scheme a fine tuning via an initial pilot simulation procedure is required. For each parameter in the model we readjust the current proposal scales by iteratively running the simulations algorithm for an initial N iterations and then calculating the mean acceptance ratio for the updates. For any parameter with a mean acceptance ratio less than 0.1, we halve the current proposal standard deviation while for any parameter with a mean acceptance probability between 0.1 and 0.2 we scale the current proposal standard deviation with a factor 0.75. For any parameter with a mean acceptance ratio between 0.4 and 0.5 we multiply the current proposal standard deviation by 1.25 and, finally, if the mean acceptance probability is greater than 0.5, we multiply the current proposal standard deviation by 1.5. This process is continued until three successive pilot runs have all mean acceptance ratios within $(0.2; 0.4)$, see Gelman et al. (1996). Note that the last visited state serves as initial state for the next pilot run. For each of these pilot simulations, a value of $N = 1\,000$ iterations appears to perform well.

4.4 Simulation Study

In order to employ the proposed Bayesian approach to assessment of the insulin secretion rate we conduct a brief simulation study in which several simulated data sets are analysed and the estimated insulin secretion rate compared to the known true rate. Thus we construct various artificial data sets with both varying number of gamma densities used in the representation of the insulin secretion rate and model parameters. In order to initiate the simulation study we need adequate prior and proposal distributions. The priors are specified according to Section 3 using prior knowledge from Watanabe et al. (1998) (see Table 1 for further details). The iterative way of both finding good starting values and achieving adequate proposal variances described above was conducted for each set of simulated data. Having obtained good proposal variances a final run of 50 000 iterations was performed. For all data sets we found very good agreement between the estimated insulin secretion rate and the true rate. Parameter estimates were also consistent and rather accurate.

PARAMETER	DISTRIBUTION
K	Geom(0.95)
κ	$\mathcal{U}(0, 100)$
m_k	$\mathcal{U}(0, 1000)$
v_k	$\mathcal{U}(0, 10000)$
w_k	$\mathcal{U}(-100, 100)$
K_I	$\mathcal{N}(0.2, 1/100)$
K_C	$\mathcal{N}(0.1, 1/100)$
K_{12}	$\mathcal{N}(0.12, 1/100)$
K_{21}	$\mathcal{N}(0.03, 1/100)$
V_{12}	$\mathcal{N}(1, 1)$
I^b	$\mathcal{N}(0.03, 1/100)$
C_1^b	$\mathcal{N}(0.5, 1/16)$
τ_I	$\Gamma(0.001, 0.001)$
τ_{C_1}	$\Gamma(0.001, 0.001)$
τ_{C_2}	$\Gamma(0.001, 0.001)$
τ_r	$\Gamma(0.001, 0.001)$
τ_{I^o}	$\Gamma(0.05, 0.01)$
$\tau_{C_1^o}$	$\Gamma(0.5, 0.01)$

Table 1: Prior distributions.

In the next section, we consider the performance of the proposed approach and present the results of our data analysis, including standard Markov chain convergence diagnostics, parameter estimates and the obtained insulin secretion rates.

5 RESULTS

The insulin secretion rate reconstruction method is applied to IVGTT data recorded from six healthy young subjects. Following an overnight fast, a glucose bolus were administered at time zero. For determination of basal levels of insulin, c-peptide and glucose in the blood plasma, blood samples were collected at times -60, -45, -30 and -15 minutes prior to the bolus. Subsequently blood samples were taken at 0, 1, 3, 5, 7, 9, 12, 15, 20, 25, 30, 45, 60, 75, 90, 105, 120, 140, 160, 180, 200, 220 and 240 minutes for measurement of insulin, c-peptide and glucose concentrations in blood plasma. These observation times constitutes $\mathcal{T}$. Regarding the resolution of process Ψ we let

$$\Lambda = \{0, 0.5, 1, 1.5, \ldots, 20, 21, 22, \ldots, 110, 112, 114, \ldots, 240\}.$$

Consequently the discretisation becomes gradually more and more coarse and need not necessarily to be equidistant. The data recorded for subject 1 is displayed in Figure 1, whereas data for all six subjects are shown in Figure 6.

Following the method outlined in Section 4; we (1) find good proposal distributions for each subject by repeatedly running a trial run for $1\,000$ iterations until all quantities needing updating obtained acceptance probabilities between $(0.2; 0.4)$; and (2) run a final Markov chain for $200\,000$ iterations. Note that the applied proposal distributions are allowed to vary between subjects as we do not impose any population constraints.

It is important to investigate the performance of the developed MCMC simulation algorithm to ensure that the obtained chain have settled to the posterior distribution and, in addition, that a sufficiently long sample have been produced allowing for reliable statistical inference. There

are at least two issues to contemplate here. Firstly, the chain may take some time to reach its stationary distribution and typically samples from this initial part of the chain is neglected. Numerous sophisticated techniques for testing the convergence of a Markov chain have been proposed in the literature and we exploit the spectral method of Geweke (1992) implemented in the CODA package (Plummer et al., 2005) for R/Splus. Secondly, having converged to its stationary distribution the chain needs to be run for sufficiently many iterations to allow for adequate statistical inference. To ensure this we propose the Heidelberger and Welch's convergence criteria (Heidelberger and Welch, 1981). See Brooks and Gelman (1998) and Brooks and Guidici (2000) for a general review of diagnostic techniques for MCMC simulation.

The output from the six MCMC simulation algorithms consist of samples from the model parameters Ω and the latent process Ψ. These subject dependent samples were all closely inspected for convergence with the spectral method of Geweke and it was found, as expected, that each of the six chains has reached burn-in at the very beginning. Consequently we assume that the final six Markov chains all have been initiated in their stationary distributions and use all $200\,000$ iterations for statistical inference. Figure 4 displays output details for some of the parameters concerning subject 1 and from here we conclude that the Markov chain appear to exhibit excellent mixing properties. Output from the remaining five subjects exhibit similar behaviour. In addition, each of the parameters of interest was also examined with the method of Heidelberg and Welch to ensure that each of the six chains have run long enough to obtain reliable inference.

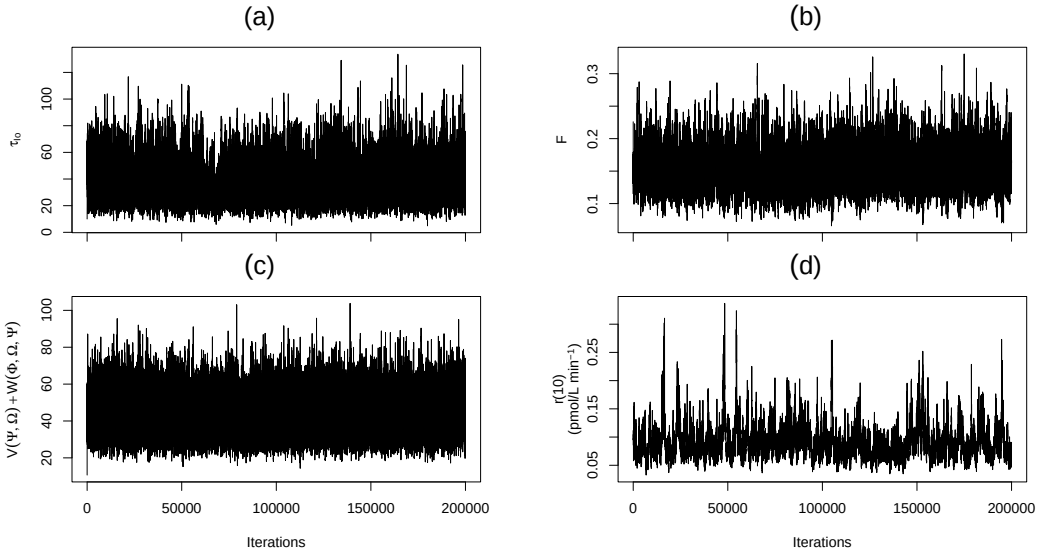

Figure 4: Trace plots for subject 1: (a) the precisions τ_{I^o}; (b) the rate F; (c) the sum of the posterior potentials $V(\Psi, \Omega) + W(\Phi, \Omega, \Psi)$; and (d) the insulin secretion rate at time $t = 10$ minutes.

Note that Figure 4(b) displays F, which can be computed from $F = f \cdot V_I/V_{C_1} = K_I I^b V_I/(K_C C_1^b V_{C_1})$, whenever the distribution volumes are known. Unfortunately these quantities are unidentifiable from this experiment, however, they may be estimated on the basis of the subject's body characteristics. Following Watanabe et al. (1998) we estimate the distribu-

tion volume for C_1 by $V_{C_1} = 0.0602 \cdot$ body weight, whereas Campioni et al. (2004) provides a method for estimating the insulin distribution volume as $V_I = \exp(0.5358 \cdot \text{BSA} + 1)$, where BSA denotes the subject's body surface area. However, the body surface area has not been recorded and is subsequently estimated by the Mosteller formula (Mosteller, 1987) as

$$\text{BSA} = \sqrt{\text{height} \cdot \text{weight}}/60.$$

From these estimates of V_{C_1} and V_I we may infer on F and obtain results indicating that approximately $80 - 85$ per cent of the secreted insulin is absorbed by the liver. See Table 2 for further details.

Parameter	Subject					
	1	2	3	4	5	6
K	2	4	2	2	3	2
K_I	$0.159_{(0.110;0.227)}$	$0.116_{(0.078;0.152)}$	$0.137_{(0.052;0.317)}$	$0.198_{(0.101;0.320)}$	$0.207_{(0.108;0.354)}$	$0.181_{(0.097;0.307)}$
K_C	$0.045_{(0.033;0.065)}$	$0.023_{(0.020;0.026)}$	$0.071_{(0.032;0.170)}$	$0.056_{(0.035;0.088)}$	$0.093_{(0.048;0.169)}$	$0.062_{(0.036;0.104)}$
K_{12}	$0.052_{(0.001;0.162)}$	$0.018_{(0.010;0.025)}$	$0.062_{(0.001;0.196)}$	$0.096_{(0.015;0.219)}$	$0.104_{(0.008;0.244)}$	$0.081_{(0.003;0.223)}$
K_{21}	$0.219_{(0.083;0.375)}$	$0.001_{(0.000;0.002)}$	$0.188_{(0.057;0.359)}$	$0.172_{(0.056;0.318)}$	$0.155_{(0.032;0.320)}$	$0.201_{(0.077;0.353)}$
V_{12}	$1.006_{(0.809;1.203)}$	$0.952_{(0.794;1.116)}$	$0.910_{(0.751;1.094)}$	$1.101_{(0.906;1.293)}$	$1.050_{(0.856;1.244)}$	$0.970_{(0.776;1.165)}$
I_b	$0.016_{(0.015;0.018)}$	$0.028_{(0.026;0.030)}$	$0.066_{(0.065;0.066)}$	$0.029_{(0.026;0.032)}$	$0.080_{(0.074;0.086)}$	$0.031_{(0.031;0.031)}$
C_b	$0.222_{(0.209;0.235)}$	$0.401_{(0.375;0.428)}$	$0.530_{(0.529;0.531)}$	$0.403_{(0.383;0.424)}$	$0.596_{(0.554;0.637)}$	$0.310_{(0.309;0.310)}$
F	$0.151_{(0.104;0.209)}$	$0.208_{(0.164;0.262)}$	$0.139_{(0.086;0.220)}$	$0.136_{(0.074;0.229)}$	$0.198_{(0.124;0.298)}$	$0.175_{(0.106;0.275)}$
τ_I	$72532_{(61254;83811)}$	$82039_{(70684;93399)}$	$86180_{(74169;98175)}$	$68241_{(56218;80253)}$	$62159_{(50117;74173)}$	$60556_{(49382;71717)}$
τ_{C_1}	$9948_{(8373;11532)}$	$9860_{(8080;11629)}$	$4886_{(2433;7249)}$	$10491_{(8392;12612)}$	$6471_{(5479;7466)}$	$9669_{(7851;11478)}$
τ_{C_2}	$54691_{(48150;61209)}$	$43095_{(35437;50734)}$	$62341_{(57946;66741)}$	$60376_{(53662;67092)}$	$53710_{(49375;58088)}$	$64515_{(57271;71704)}$
τ_r	$19151_{(15113;21171)}$	$12124_{(10299;13921)}$	$21811_{(20461;23150)}$	$19039_{(15991;22063)}$	$25881_{(24221;27553)}$	$22528_{(21199;23850)}$
τ_{I^o}	$22.3_{(12.7;39.1)}$	$62.2_{(32.0;106.0)}$	$25.1_{(11.6;44.3)}$	$17.6_{(8.0;31.4)}$	$49.9_{(20.8;95.7)}$	$19.1_{(9.0;33.4)}$
$\tau_{C_1^o}$	$12.6_{(4.9;23.3)}$	$82.1_{(35.2;144.9)}$	$89.2_{(39.7;161.4)}$	$206.4_{(93.5;364.5)}$	$95.1_{(39.6;179.9)}$	$147.3_{(63.9;266.6)}$

Table 2: The achieved posterior mean estimates together with 95 per cent credible intervals for the six subjects.

From the samples obtained from the Markov chains the corresponding posterior densities may also be computed. Figure 5 gives the posterior density for some of the parameters for subject 1 with the applied priors superimposed. Table 2 provides the obtained subject dependent parameter characteristics.

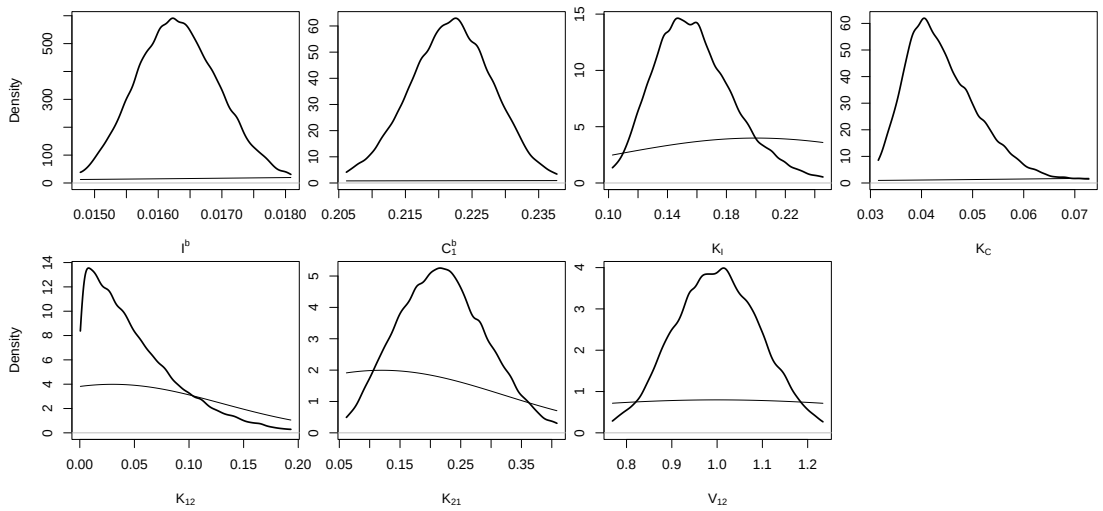

Figure 5: Posterior densities (bold lines) for the parameters I_b, C_b, K_I, K_C, K_{12}, K_{21} and V_{12} for subject 1. Superimposed in thin lines are the applied prior densities.

Note that Figure 4(d) provides the visited states of the insulin secretion rate $r(t)$ at time $t = 10$ minutes. Here the insulin secretion rate is measured in pmol/(L min) as $r(t)$ is relative to the C_1 distribution volume. In order to determine the actual insulin secretion $R(t) = V_{C_1} r(t)$, we thus need to rescale with V_{C_1}. However, in order to allow for a comparison across subjects we consider only $r(t)$, which is assessed by computing the posterior mean and constructing the corresponding 95 per cent credible intervals for any $t \in \Lambda$. See Figure 6 where also posterior mean curves and 95 per cent credible intervals for $I(t)$ and $C(t)$ are provided.

From Figure 6 we see that the proposed simulation algorithm provides realistic time-continuous estimates of the insulin secretion rate compared to Watanabe et al. (1998), where $r(t)$ is considered as piecewise constant. We observe similar patterns for all six subjects as the insulin secretion is characterized by a pronounced first phase insulin secretion and then followed by a moderate second phase insulin secretion.

Having obtained an efficient and flexible technique for assessing the insulin secretion rate we need investigate the influence of the imposed prior distribution. Thus we perform a prior sensitivity analysis where univariate marginal likelihoods are computed for each subject dependent parameter by simply dividing the posterior distribution by the applied prior distribution. See Figure 7 for marginal likelihood functions for the parameters reported in Figure 5. It is apparent that the prior is not being to dominating in the posterior, since the marginal likelihood functions are non-constant functions of the parameters under investigation. Marginal likelihood functions for the remaining parameters for the other subjects exhibit similar behaviour. Thus we conclude that the prior used is not too restrictive and that the information inherent in the likelihood is properly accounted for.

6 Discussion

In this paper, we develop and discuss a practical Bayesian approach for estimation of the prehepatic insulin secretion rate. A superposition of gamma densities serves as a flexible model of the insulin secretory rate in the extended combined two-compartment C-peptide model. Traditionally this has been modelled as a piecewise constant function, see e.g. Watanabe et al. (1998). This combined model allows for assessment of the prehepatic insulin secretion rates from a single experiment, whereas alternative methods rely upon a two-stage experimental protocol. See e.g. Sparacino and Cobelli (1996) and Andersen and Højbjerre (2005*b*).

The introduction of the two-compartmental C-peptide kinetics in the extended combined model leads to an ill-posed estimation problem, which previously has been solved by oscillating between using insulin and C-peptide measurements as forcing functions (Sparacino and Cobelli, 1996). This iterative procedure for identifying the insulin secretory rates and kinetics parameters is not truly simultaneous. We propose an alternative fully Bayesian approach to analyzing C-peptide and insulin data simultaneously by recasting the differential equations in the extended combined model as stochastic processes in a complex graphical model. This unified graphical model representation of the extended combined model relates the C-peptide data to insulin data via the insulin secretion rate. Furthermore, the graphical model includes two distinct types of variability; (1) noise on the actual observations and (2) noise on the latent processes. The latter type of variability allows the current physiological state of the subjects to influence on the processes.

The application of reversible jump MCMC methodology allows for efficient and reliable

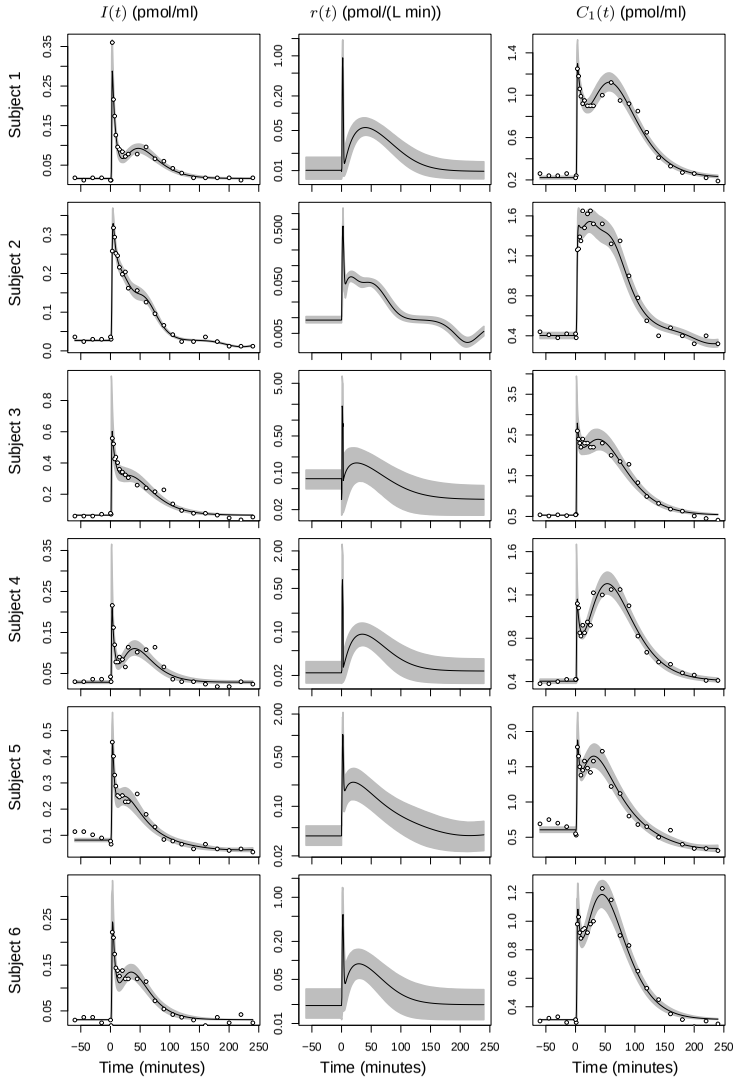

Figure 6: Posterior mean (black line) and 95% credible intervals superimposed in gray from top to bottom for six healthy subjects and from left to right for $I(t)$, $r(t)$ and $C(t)$ following a glucose bolus injection in an IVGTT.

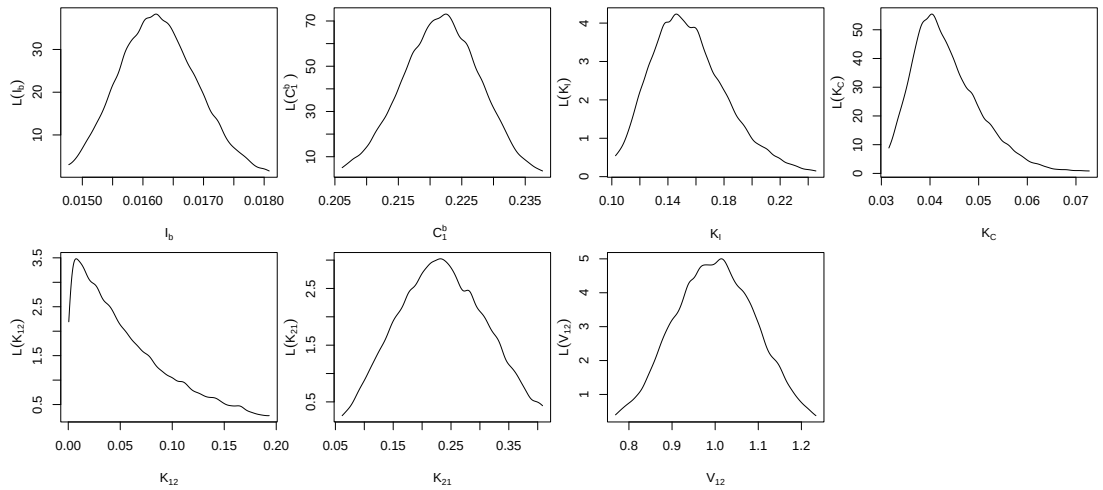

Figure 7: Marginal likelihood functions for the parameters I_b, C_b, K_I, K_C, K_{12}, K_{21} and V_{12} for subject 1.

posterior inference on the complete kinetic profile of the prehepatic insulin secretory system. In addition, adequate inference about important physiological characteristics as e.g. the insulin surviving extraction in liver F and the two elimination constants K_I and K_C has become possible. Consequently the analysis presented here is the first analysis of C-peptide and insulin data from a glucose tolerance test to properly account for simultaneous identification.

The model presented is currently being integrated into a population based approach to the minimal model of glucose and insulin homeostasis (Bergman et al., 1979; Toffolo et al., 1980). The minimal model relates the glucose and insulin processes via a latent active insulin process, see e.g. Andersen and Højbjerre (2005*a*) for a recent fully Bayesian analysis of the minimal model in a population based setting. However, combining the two distinct models into a complete unified graphical model introduces several new quantities to be assessed. Nevertheless, the available glucose data provide additional information which may be utilized for establishing an improved characterization of the pathogenesis of non-insulin dependent diabetes mellitus.

Acknowledgments

We would like to thank Professor Claudio Cobelli, Department of Information Engineering, University of Padova, Italy, for kindly providing the data. We are indebted to Poul Svante Eriksen and Bjarne Højgaard, Aalborg University, and Aage Vølund, Novo Nordisk A/S, for inspiring discussions and helpful comments.

REFERENCES

Andersen, K. E. and Højbjerre, M. (2005*a*), 'A population-based Bayesian approach to the minimal model of glucose and insulin homeostasis', *Statistics in Medicine* **24**, 2381 – 2400.

Andersen, K. E. and Højbjerre, M. (2005*b*), Reconstructing the insulin secretion rate by

Bayesian deconvolution of phase-type densities, Technical Report R-2005-32, Aalborg University.

Bergman, R. N., Ider, Y. Z., C. R. Bowden, C. R. and Cobelli, C. (1979), 'Quantitative estimation of insulin sensitivity', *American Journal of Physiology* **236**, E667 – E677.

Brooks, S. P. (1998), 'Markov chain Monte Carlo method and its application', *The Statistician* **47**, 69 – 100.

Brooks, S. P. and Gelman, A. (1998), 'General methods for monitoring convergence of iterative simulations', *Journal of Computational Graphical Statistics* **7**, 434 – 455.

Brooks, S. P. and Guidici, P. (2000), 'MCMC convergence assessment via two-way ANOVA', *Journal of Computational Graphical Statistics* **9**, 266 – 285.

Campioni, M., Toffolo, G., Rizza, R. and C., C. (2004), 'Estimation of hepatic insulin extraction during IM–IVGTT: Individual vs standard kinetic parameters', *International Federation for Medical & Biological Engineering News* **68**, 36 – 39.

Eaton, R. P., Allen, R. C., Schade, D. S., Erickson, K. M. and Standefer, J. (1980), 'Prehepatic insulin production in man: Kinetic analysis using peripheral connecting peptide behaviour', *Journal of Clinical Endocrinology Metabolism* **51**, 520 – 528.

Faber, O. K., Kehlet, H., Madsbad, S. and Binder, C. (1978), 'Kinetics of human c-peptide in man', *Diabetes* **27 (Suppl.1)**, 207 – 209.

Gelman, A., Roberts, G. O. and Gilks, W. R. (1996), Efficient Metropolis jumping rules, *in* J. M. Bernardo, J. O. Berger, A. P. Dawid and A. F. M. Smith, eds, 'Bayesian Statistics 5', New York: Oxford University Press, pp. 599 – 608.

Geweke, J. (1992), Evaluating the accuracy of sampling-based approaches to calculating posterior moments, *in* J. Bernado, J. Berger, A. Dawid and A. Smith, eds, 'Bayesian Statistics 4', Clarendon Press, Oxford, UK.

Green, P. J. (1995), 'Reversible jump MCMC computation and Bayesian model determination', *Biometrika* **82**, 711–732.

Hadamard, J. (1923), 'Lectures on the Cauchy Problem in Linear Partial Differential Equations', Yale University Press, New Haven.

Heidelberger, P. and Welch, P. D. (1981), 'A spectral method for confidence interval generation and run length control in simulations', *Communications of the Association for Computing Machinery* **24**, 233 – 245.

Hovorka, R. (1993), 'A computer program to reconstruct insulin secretion', *Diabetologia* **36 (Suppl.1)**, A68.

Hovorka, R., Patel, J., Lettis, S., Pirjamali, R., Young, M. A. and Eckland, D. J. A. (1994), 'Reproducibility of pre-hepatic insulin secretion during IVGTT', *Diabetologia* **37 (Suppl.1)**, A126.

Hovorka, R., Soons, P. A. and Young, M. A. (1996), 'ISEC: a program to calculate insulin secretion', *Computer Methods and Programs in Biomedicine* **50**, 253 – 264.

Kjems, L. L., Vølund, A. and Madsbad, S. (2001), 'Quantification of beta-cell function during IVGTT in type II and non-diabetic subjects: assessment of insulin secretion by mathematical methods', *Diabetologia* **44**, 1339 – 1348.

Lauritzen, S. L. (1996), *Graphical Models*, Oxford: Clarendon Press.

Mosteller, R. D. (1987), 'Simplified calculation of body surface area', *New England Journal of Medicine* **317**(17), 1098.

Plummer, M., Best, N., Cowles, K. and Vines, K. (2005), *CODA: Convergence diagnostics and output analysis software for Gibbs sampling output*, Version 0.10-2, MRC Biostatistics Unit, Cambridge, UK.

Poland, W. B. and Shachter, R. D. (1994), Three approaches to probability model selection, *in* R. Lopez de Mantaras and D. Poole, eds, 'Uncertainty in Artificial Intelligence: Proceedings of the Tenth Conference', pp. 478 – 483.

Robert, C. P. and Casella, G. (1999), *Monte Carlo Statistical Methods*, Springer-Verlag, New York.

Sparacino, G. and Cobelli, C. (1996), 'Stochastic deconvolution method to reconstruct insulin secretion rate after a glucose stimulus', *IEEE Transactions on Biomedical Engineering* **43**, 512 – 529.

Toffolo, G., Bergman, R., Finegood, D., C.R., Bowden and Cobelli, C. (1980), 'Quantitative estimation of beta cell sensitivity to glucose in the intact organism: a minimal model of insulin kinetics in the dog', *Diabetes* **29**, 979 – 990.

Vølund, A., Polonsky, K. and Bergman, R. N. (1987), 'Calculated pattern of intraportal appearance without independent assessment of c-peptide kinetics', *Diabetes* **36**, 1195 – 1202.

Watanabe, R. M. and Bergman, R. N. (2000), 'Acurate assessment of endogenous insulin secretion does not require seperate assessment of c-peptide kinetics', *Diabetes* **49**, 373 – 382.

Watanabe, R. M., Steil, G. M. and Bergman, R. N. (1998), 'Critical evaluation of the combined model approach for estimation of pre-hepatic insulin secretion', *American Journal of Physiology* **274**, E172 – E183.

Watanabe, R. M., Vølund, A., Roy, S. and Bergman, R. N. (1989), 'Prehepatic β-cell secretion during the intravenous glucose tolerance test in humans:application of a combined model of insulin and c-peptide kinetics', *Journal of Clinical Endocrinology Metabolism* **69**, 790 – 797.